Histopathological Evaluation of Anti-Atherosclerosis Activity of *Terminalia Catappa in vivo*

Doris Tabansi
Modibbo Adama University of Technology
Daniel Dahiru
Modibbo Adama University of Technology
Ambrose Teru Patrick
Modibbo Adama University of Technology
Faith Pwaniyibo Samson
Modibbo Adama University of Technology
Wan Jin Jahng
wan.jahng@gmail.com

Julia Laboratory https://orcid.org/0000-0001-8241-7739

Research Article

Keywords: atherosclerosis, medicinal plant, Terminalia catappa, atherogenic diet, interactome, metabolomics, proteomics

Posted Date: March 10th, 2026

DOI: https://doi.org/10.21203/rs.3.rs-9067509/v1

Additional Declarations: The authors declare no competing interests.

Abstract

The current study determined the anti-atherosclerotic activity of *Terminalia catappa* using a diet-induced murine model in vivo. Our in vivo murine model using atherogenic diet induced atherosclerosis. Histological examinations of the diet-induced atherosclerosis indicated an atherogenic-related phenotype. Treatment with *Terminalia catappa* decreased cholesterol deposits in the lumen of the blood vessels in the aorta, heart, and liver. Protein interactome and metabolomic network in this study imply potential mechanisms and biomarkers of atherosclerosis. Protein interactome demonstrated that actin is the central switch of atherosclerosis through plaque rupture, thrombosis, macrophage, and cystic fibrosis as potential pathogenic mechanisms. Metabolome mapping reveals that cholesterol metabolism is directly connected to the aromatic amino acid pathway, fatty acids, lysophosphatidylcholine, citric acid, creatine, and cholic acid metabolism. The current study suggests the comprehensive functional profiles of atherosclerosis mechanisms. Our results propose that *Terminalia catappa* has the potential to cease the progression of atherosclerosis.

Introduction

Atherosclerosis is a multifactorial chronic disease of plaque formation in the arteries.[1] Diverse determinants demonstrated that hemodynamics, lipid concentration, smoking, inflammation, and energy imbalance positively correlate with the disease, indicating a heterogeneous molecular profile.[2] Prevention of atheromatous lesions is a critical target in the prophylaxis and cardiocirculatory disorders with atherothrombotic complications.[3] Atherosclerosis is an inflammatory condition leading to the development of ischemic heart diseases, cerebrovascular diseases, and peripheral vascular diseases.[4] However, atherosclerosis initiation, progression, and termination are elusive at the molecular level.[5] We introduced an in-depth analysis of the aorta, heart, and liver using histopathology, proteomics, and metabolomics to identify significant components of atherosclerosis. In addition, we analyzed histopathology using the atherogenic-diet-induced murine model in vivo, followed by pharmacological rescue experiments.

Hyperlipidemia leads to the early development of atherosclerosis and cardiovascular complications.[6] Incipient lipid accumulation in the artery wall initiates inflammatory signaling.[7] Endothelium was modified through a local prothrombotic balance and inflammatory responses.[8]Endothelial injury is induced by low-density lipoprotein cholesterol (LDL-C) oxidation and initiates the expression of proinflammatory biomarkers.[9]

Terminalia catappa (Combretaceae) is a medicinal plant listed as a pharmacopeia vegetable in Asia and Africa.[12] Our previous in vivo study demonstrated that *Terminalia catappa* extracts could regulate total cholesterol (TC), total triglycerides (TG), low-density lipoprotein cholesterol (LDL-C), and very low-density lipoprotein cholesterol (VLDL-C). In addition, ametabolic biomarkers, including alanine transaminase, aspartate aminotransferase, alkaline phosphatase, creatine kinase, and lactate dehydrogenase,

decreased using *Terminalia catappa* extracts. In the current study, we determined the anti-atherosclerotic roles of *Terminalia catappa* extracts in a diet-induced murine model based on histopathology and protein/metabolite interactome mapping. The current study demonstrated that the *Terminalia catappa* fruit extracts decreased cholesterol deposits in the lumen of the blood vessels in the heart, aorta, and liver, shown by quantitative histological analysis.

Previously, our quantitative analysis data indicated that *T. catappa* contains substantial amounts of phenols, alkaloids, flavonoids, cardiac glycosides, and saponins. Atherogenic diet-induced atherosclerosis was confirmed by a significant elevation in serum levels of TC, TG, LDL-C, VLDL-C, and a decreased HDL-C compared to standard diet control. Concomitant administration by gastric intubation of *Terminalia catappa* extracts and an atherogenic diet significantly suppressed the progression of atherosclerosis by reducing TC, TG, LDL-C, and VLDL-C as increasing HDL cholesterol. In addition, increased activities of ALT, AST, ALP, CK, and LDH under an atherogenic diet were significantly reversed with ETC and ATC treatment. The efficacy of *Terminalia catappa* is compatible with Atorvastatin as the positive control.

The proteome and metabolome map shows that the pathogenesis of atherosclerosis is connected to hyperlipidemia and hypercholesterolemia-induced unwavering energy disturbances, inflammation, and oxidative stress. It is unarguable that atherosclerosis also occurs in some patients whose lipid level is well-controlled, suggesting that other pathogenic factors may contribute to the phenomenon.

The current proteome and metabolome map demonstrates: (1) β-actin is a central regulator of atherosclerosis, (2) a positive correlation exists between cystic fibrosis, and atherosclerosis, (3) proteins and metabolites of thrombosis, plaque rupture, macrophages are essential players of atherosclerosis. Atherosclerosis begins with an early inflammatory reaction, including an imbalance in energy metabolism and an immune response induced by macrophages in the artery. The current interactome indicates that altered lipid and glucose homeostasis may lead to energy imbalance, initiating the primary atherosclerosis reactions.

We demonstrated that ethanolic and aqueous extracts of *Terminalia catappa* fruit exhibited anti-atherosclerotic, anti-hyperlipidemic, and hypolipidemic activity in atherogenic diet-induced atherosclerosis in vivo.

Materials and Methods

Atorvastatin, cholic acid, and cholesterol were obtained from Sigma-Aldrich, Milwaukee, WI, US. All other chemicals were analytical grade.

Plant materials

Terminalia catappa Linn (T. catappa) fruits were obtained from Jimeta, Adamawa State, Nigeria, in February 2015 (latitude 11055'N and longitude 11011'). Dr. Bristone B. and Professor Chimbe Konje,

plant taxonomists, confirmed the identity of the herbarium specimens using taxonomic literature. The fruit was preserved and deposited in the herbarium of Modibbo Adama University, Yola, Nigeria, with the voucher number MAU/YL/BT/0420, providing a pressed, mounted sample for future research.

Animals

Male Wistar/albino rats (200–250 g, 7 weeks old) were procured from the Veterinary Research Institute in Vom, Jos, Nigeria and housed five rats per cage. Animals were maintained on a standard diet from Vital Feeds (Jos, Nigeria) and provided with *ad libitum* access to freshwater for six weeks. Before the commencement of the experiment, a one-week acclimatization period to laboratory conditions was allowed. Atherosclerosis was induced by administering an atherogenic diet containing 1.25% cholesterol, 0.5% cholic acid, 1 5% fat, and 83.25% standard pellet. All animal experiments adhered to the guidelines outlined in the 8th edition of the "Guide for the Care and Use of Laboratory Animals" (2006, NIH). The protocols were approved by the Animal Experimental Ethics Committee of the Modibbo Adama University of Technology under approval number UAEC/YMAU/YL/0100 on January 4th, 2016, in accordance with NIH guidelines for the care and use of laboratory animals.

Terminalia catappa fruit extraction

Terminalia catappa was prepared by slicing and shade drying to remove moisture, followed by pulverization into a powder. This powder was then macerated in either ethanol or distilled water, filtered, and concentrated to obtain semi-dried brown solids, which were stored in refrigeration. Post-extraction drying methods included lyophilization or oven-drying, with variations in temperature and duration depending on the solvent used for extraction.

Histopathological determination

For histological investigations, specimens of the liver, heart, and aorta were preserved in 10% buffered formaldehyde solution, followed by sectioning, and embedding in paraffin wax using standard methods.[13] The heart and liver were then sliced transversely at the arch and mid-thoracic levels. The tissues were then fixed in Bruin's solution for a whole day before being subjected to a standard histological analysis using graded alcohols. Using a microtome, tissue sections (6–8 µm thick) were cut, placed on glass slides, and stained with hematoxylin and eosin. A light microscope (Optinity KB-600 microscope) and a digital camera (Optinity KCS3-3200SS, 32MP Exmor Sony Cmos Sensor) were used to evaluate the tissue samples.

Construction of PPI network

Around one thousand proteins in the aorta, liver, and heart were identified. Psort (http://psort.ims.utokyo.ac.jp/) and TargetP (http://www.cbs.dtu.dk/service/TargetP/) algorithms were

used to demonstrate the subcellular localization of a given protein in the aorta, heart, and liver to filter out false positives. Atherosclerotic proteins were included in the positive control list. The atherogenic protein interactome was established using PPI software STRING 11 (http//:string-db.org/) by adding 1,000 identified proteins in the query. Protein interactome map demonstrated eight potential interactions, including neighborhood (green), gene fusion (red), co-occurrence (dark blue), coexpression (black), binding experiment (purple), database (blue), text mining (lime), and homology (cyan). Aorta, heart, and liver proteins were collected based on their accession number, gene name, protein name, and model type as selection criteria. All proteins in the aorta, heart, and liver were validated using the UniProt Knowledgebase (UniProtKB). For atherosclerotic proteins, we collected > 200 interacting proteins identified in atherosclerosis (Supporting Information Table S1). The proteins were identified using the Database of Interacting Proteins (DIP), Human Protein Reference Database (HPRD), European Molecular Biology Laboratory (EMBL)-European Bioinformatics Institute (EBI), and protein sequences of these genes were obtained using FASTA (protein and DNA sequence alignment software package) from NCBI (National Center for Biotechnology Information, http://www.ncbi.nlm.nih.gov/). For the metabolomics mapping, all known metabolites in atherosclerosis were analyzed using bioinformatics tools, including OmicsNet software (https://www.omicsnet.ca/). OmicsNet is a visual network system to create a network relationship among genes, proteins, miRNAs, metabolites, or transcription factors in three-dimensional (3D) space. Hundereds metabolites in atherosclerosis were connected to aromatic acids, creatine, succinic acid, APOE, citric acid, fucose, cholic acid, cholesterol, fatty acids, sphinganine, DHA and lysoPC (Supporting Information Table S5). The metabolites were validated using their PubChem and KEGG (Kyoto Encyclopedia of Genes and Genomes) identification number (https://pubchem.ncbi.nlm.nih.gov/rest/pug). A comprehensive metabolome map (metabolite-protein interaction) was established using an Omicsnet algorithm. The metabolome map validated the protein interactome to uncover hidden interactions and molecular mechanisms. Further, using STRING software, the proteins obtained from the metabolome map were used to generate the metabolite-protein interactome network to elucidate the metabolite-related protein network.

Results

To determine the anti-atherosclerotic effects of *Terminalia catappa*, we examined the aorta, heart, and liver tissues of the atherogenic diet/plant extracts-treated rats. Aorta from atherogenic diet-induced rats showed the major arterial vessel with atrophic endothelial and smooth muscles and cholesterol plaques in the lumen (Fig. 1). Under standard diet control, tissues showed a major arterial vessel with a free lumen containing blood cells and intima of the endothelium free of any lipid deposit surrounding the adventitial layer (Fig. 1A). The plaques in the atherogenic group occlude over 40% of blood passage (Fig. 1B). Administration of standard drug (Fig. 1C, Atorvastatin 10 mg/kg) under atherogenic condition showed a lumen containing much-reduced cholesterol deposits with blood cell clusters.[22]

Terminalia catappa ethanol extracts (100 mg/kg) with an atherogenic diet indicated major arterial vessels showing adventitia layers, endothelium, and fibrous media,. The lumen contains a certain

amount of cholesterol plaques and clusters of blood cells. The plaques occlude part of the endothelial surface, narrowing 30% of blood passage (Fig. 2). Administration of *Terminalia catappa* (Fig. 1E, 200 mg/kg ethanol extracts) with an atherogenic diet shows a major arterial vessel with endothelium, fibrous media, and adventitia layers; the lumen contains less amount of cholesterol plaques occluding 20% of blood passage. Administration of a higher concentration of *Terminalia catappa* (Fig. 1F, 300 mg/kg of ethanol extracts) with an atherogenic diet shows major arterial vessels with endothelium, fibrous media, and adventitia layers. In addition, the lumen contains much-decreased levels of cholesterol plaques with a 5% narrowing of blood passage.

Co-administration of *Terminalia catappa* aqueous extracts (Fig. 1G, 100 mg/kg ATC) and atherogenic diet showed hepatocyte tissue with coronary arteries of the endothelium, fibrous media, and adventitia layers. The lumen contains cholesterol plaques and blood cell clusters. The plaques occlude the endothelial surface with 30% narrowed blood passage. Aqueous extracts with an atherogenic diet (Fig. 1H, 200 mg/kg ATC) show cholesterol plaques occluding the endothelium with 20% narrowed blood passage (Fig. 2, Supporting Information Table S6). Higher concentrations of aqueous extracts of *Terminalia catappa* (Fig. 1I, 300 mg/kg ATC) showed much-decreased cholesterol plaques with 10% reduced blood passage. With positive control, the intima of the endothelial surface is free of plaques with no occlusion of blood passage. Under standard diet conditions, *Terminalia catappa* (Fig. 1J, 300 mg/kg ETC; Fig. 1K, 300 mg/kg ATC) shows major arterial vessels with free lumen-containing blood cells and no lipid deposits in their intima.

Heart sections of the atherogenic group showed cardiac tissue with coronary arteries containing massive cholesterol plaques (Fig. 1M). The cholesterol plaques occlude up to 70% of blood passage, while the standard diet condition shows healthy cardiac tissue with coronary arteries containing free blood cells (Fig. 1L). In addition, the intima is free of any lipid deposits.

Terminalia catappa treatment (100 mg/kg ETC) under an atherogenic diet shows cardiac tissue with coronary arteries containing milder cholesterol plaques and blood cell clusters in the lumen (Fig. 1N). The cholesterol plaques occlude part of the endothelial surface with 20% reduced blood passage. *Terminalia catappa* extracts (200 mg/kg ETC) demonstrated dose-dependent anti-atherosclerotic effects indicating cardiac tissue with coronary arteries containing much-reduced cholesterol plaques and blood cell clusters with 20% narrowed blood flow (Fig. 1O). The highest dose of *Terminalia catappa* (300 mg/kg ETC with an atherogenic diet) shows minimum cholesterol plaques in the coronary artery and increased blood clusters in the lumen (Fig. 1P). In addition, the cholesterol plaques occlude part of the endothelial surface with less than 4% narrowing of blood passage. All histopahological data were analyzed quantitatively (Fig. 1Q, Supporting Information Table S6).

The *Terminalia catappa* treatment effect on the cardiac tissue was determined. Histological examination of *Terminalia catappa* treatment (Fig. 2A, 300 mg/kg ETC; Fig. 2B, 300 mg/kg ATC) under a standard diet (Fig. 2C) showed healthy cardiac tissue. Co-administration of *Terminalia catappa* extracts (100 mg/kg ATC) with an atherogenic diet shows cardiac tissue with coronary arteries containing mild cholesterol

plaques and blood cell clusters in the lumen (Fig. 2D). The cholesterol plaques occlude most endothelial surfaces with a 30% narrowing of blood passage. An increased dose of plant extracts (200 mg/kg ATC with an atherogenic diet) shows cholesterol plaques occluding 20% of blood passage (Fig. 2E). The highest dose (300 mg/kg ATC with an atherogenic diet) shows about 10% occlusion of blood passage (Fig. 2F). Concomitant administration of Atorvastatin (10 mg/kg, positive control) with an atherogenic diet shows coronary arteries containing no cholesterol deposits. However, blood cell clusters exist in the lumen (Fig. 2I). The intima of the endothelium is free of plaques with no occlusion of blood passage under positive control. Administration of a standard diet with plant extracts (300 mg/kg ETC or ATC) shows healthy cardiac tissues with coronary arteries containing blood cell clusters and no lipid deposits in their intima.

Next, we examined the liver tissue of atherosclerotic rats. Histology demonstrated massive deposits of cholesterol plaques in the lumen with 70% occlusion of blood passage (Fig. 2H and 2M), while under the standard diet condition, the liver shows healthy hepatocyte tissue with blood vessels containing blood cells within the lumen (Fig. 2G). The intima of the lumen is free of any lipid deposits (Fig. 2G). Treatment with plant extracts (100 mg/kg ETC and atherogenic diet) shows moderate cholesterol plaques and blood clusters in the lumen (Fig. 2J). The cholesterol plaques occlude more than half of the endothelial surface. Dose-dependent improvement was shown that cholesterol plaques were reduced with a 40% narrowing of the blood passage in the 200 mg/kg ETC/atherogenic diet group (Fig. 2K). The highest dose (300 mg/kg ETC) decreased cholesterol plaques and improved blood passage (30% to 85%) (Fig. 2L).

Co-administration of 100 mg/kg ATC with an atherogenic diet shows liver tissue with coronary arteries containing cholesterol plaques and blood cell clusters in the lumen (Fig. 2N). The cholesterol plaques occlude most endothelial surfaces with 30% reduced blood passage. ATC (200 mg/kg) with an atherogenic diet shows cholesterol plaques blocking 20% of blood passage (Fig. 2O). The highest dose of ATC (300 mg/kg) with an atherogenic diet offers healthier liver tissue with fewer lipid deposits (Fig. 2P). Concomitant administration of Atorvastatin (10 mg/kg) with an atherogenic diet shows healthy hepatocytic tissue. The intima of the endothelium is free of plaques with no occlusion of blood passage. Quantitative analysis of *Terminalia catappa*-treated tissues was shown in Fig. 2Q. The Y-axis represents % occlusion, whereas the X-axis shows the designation of each condition.

Administration of a standard diet with 300 mg/kg ETC or ATC shows healthy hepatocytes with blood vessels containing blood clusters in the lumen, indicating no toxicity of the plant extracts to the aorta, heart, and liver. Plant extracts did not increase lipid deposits or plaques in their lumen intima.

Histopathological examinations of the aorta, heart, and liver demonstrated that atherogenic diet-induced atherosclerotic lesions formed lipid deposits and plaque in the lumen of the artery, occluding up to 40% (aorta), 70% (heart), and 70% (liver) of blood passage through the lumen respectively, compared to standard diet control (Figs. 1 and 2, Supporting Information Table S6, S7). Our experiments confirmed that co-administration of ETC and ATC (300 mg/kg) with an atherogenic diet effectively suppressed

inflammation and lipid deposits. The anti-atherosclerotic effect of organic solvent extraction was more evident than aqueous extraction in histopathological examinations. Rats treated with Atorvastatin under an atherogenic diet condition led to no cholesterol deposits in the lumen of the arteries. In addition, rats treated with ETC/ATC without an atherogenic diet showed normal histology in the aorta, heart, and liver, indicating no toxicity of plant extracts toward these organs. Our data demonstrate that *Terminalia catappa* contains molecules of anti-atherosclerotic, anti-hyperlipidemic, and hepatoprotective properties, including reduced lipid deposits and improved blood passage.

Previously, our study demonstrated that *Terminalia catappa* extracts significantly ($P < 0.05$) decreased the serum levels of total cholesterol (TC), total glycerides (TG), low-density lipoprotein (LDL), and very low-density lipoprotein (VLDL) compared to the atherogenic control rats. In addition, the activities of tissue enzyme biomarkers, including alanine transaminase (ALT), aspartate aminotransferase (AST), alkaline phosphatase (ALP), creatine kinase (CK), and lactate dehydrogenase (LDH) were also significantly ($P < 0.05$) decreased compared to atherogenic control. The current experiments demonstrated that the plant extracts improved cholesterol deposits in the lumen of the blood vessels of the aorta, heart, and liver.

Atherosclerosis interactome map

The comprehensive atherosclerosis interactome was established using atherosclerotic-specific proteins from the current study and known proteins using STRING software (Fig. 3).[23] The protein interactome map demonstrated that atherosclerosis-related proteins might influence energy imbalance, inflammation, cell cycle, cystic fibrosis, lipid concentration, and phosphorylation signaling when upregulated or downregulated under various stress conditions (Supporting Information, Table S2).

Atherosclerosis mapping revealed that lipid-mediated transcription factors and phosphorylation signaling could initiate protein signaling in atherosclerosis. The PPI map supported the idea that interacting proteins under energy imbalance could be involved in inflammation in the aorta, heart, and liver. The current study identified altered inflammation switch as the major pathological pathway determined by the atherosclerosis network. Further, the atherosclerotic interactome could identify the clinical target of inhibition for the anti-inflammatory and anti-hyperlipidemic networks (Supporting Information S3).

The atherosclerosis-specific proteins in the map were divided into six groups based on their functional regulatory roles, including k-means clustering (Supporting Information Table S4, Figure S1). Grouping the protein interactions into clusters further confirmed the sub-network on their active roles, including transcription, inflammation, lipid homeostasis, energy balance, amino acids metabolism, macrophage, and salt concentration (Fig. 3).

Protein interactome was dissected into six different subnetworks, including podosome/macrophage (Fig. 3A green; PARV, WAS, ITGA), lipid metabolism (Fig. 3B red; APOE, LPA, LCAT, APOA1, LRP1), transcription control (Fig. 3C blue; EGFR, PLCG, TRAF6, annexin V, MYD88, STAT3, p53), anion

channel/salt concentration/cystic fibrosis (Fig. 3D pink; CFTR, EREG, RICTOR), inflammation switch (Fig. 3E yellow; IL1A, ICAM1, NOS, FABP, TLR), and cell cycle (Fig. 3F black; CCNA2, CDK2, CDC6). A functional description of proteins was presented in detail (Supporting Information Table S2).

The k-means algorithm was essential due to their unsupervised clustering method based on the adjacent matrix that determines which molecules go to the group of pre-specified criteria (Supporting Information Table S4, Figure S1).

Two proteins connected by multiple lines demonstrated that interactions were derived from more than one source of information. For example, on segregating the network based on k-means clustering, the members within each cluster were highly interconnected, reflecting a functional association indicating crosstalk between networks.

Next, to understand the metabolite interactions in atherosclerosis, the metabolome map of all known metabolites was established using various bioinformatic tools, including OmicsNet software (Fig. 4, Supporting Information Table S5). Over 100 metabolites were collected from the databases that include ZINC, SMPDB, and GDB-13, followed by interactome mapping of 53 specific metabolites related to atherosclerosis to identify metabolite-proteome interactions. The metabolome map showed that molecules were interconnected to the citric acid cycle, amino acid metabolism, lysoPC, cholesterol, cholic acid, succinic acid, and creatine.

The metabolome map demonstrated that potential atherosclerosis mechanisms might include fatty acid metabolism (palmitic acid, linolenic acid, DHA), altered aromatic amino acids (phenylalanine, tyrosine, tryptophan), organic acid metabolism (succinic acid, citric acid, cholic acid), sphingolipid (sphinganine, phytosphingosine), and cholesterol (Fig. 5).

Discussion

In the current study, we determined the anti-atherosclerotic roles of *Terminalia catappa* extracts in vivo based on histopathology and protein/metabolite interactome mapping. First, we introduced an atherosclerotic animal model using atherogenic diet-induced albino Wistar rats (n = 55, 5 x 11 groups).[24] Previously, our quantitative analysis demonstrated that *Terminalia catappa* contains substantial amount of phenols, alkaloids, flavonoids, cardiac glycosides, and saponins. Atherosclerosis induced by an atherogenic diet was confirmed by a marked increase in serum levels of total cholesterol (TC), triglycerides (TG), low-density lipoprotein cholesterol (LDL-C), very low-density lipoprotein cholesterol (VLDL-C), and a decrease in high-density lipoprotein cholesterol (HDL-C) compared to rats on a standard diet.

The concurrent administration of *Terminalia catappa* extracts with an atherogenic diet via gastric intubation led to a significant inhibition of atherosclerosis progression. This effect was confirmed by reductions in total cholesterol (TC), triglycerides (TG), low-density lipoprotein cholesterol (LDL-C), and very low-density lipoprotein cholesterol (VLDL-C), coupled with an increase in high-density lipoprotein

cholesterol (HDL). Additionally, the elevated activities of alanine aminotransferase (ALT), aspartate aminotransferase (AST), alkaline phosphatase (ALP), creatine kinase (CK), and lactate dehydrogenase (LDH) were observed under the atherogenic diet with both ETC and ATC treatment, comparable to the effects of Atorvastatin as a positive control. Importantly, rats administered the highest dose of *Terminalia catappa* extracts exhibited no significant differences compared to those on a standard diet, indicating the absence of cytotoxicity.

The current histopathological data showed that atherosclerotic plaques induced by an atherogenic diet in the lumen of the aorta, heart, and liver were regressed by ETC and ATC treatment. Histopathologically, we demonstrated that ethanolic and aqueous extracts of *Terminalia catappa* fruit exhibited anti-atherosclerotic activities in atherogenic diet-induced atherosclerosis in vivo. The extract-administered groups improved the lipid profile, enzyme biomarkers, histopathology, cardioprotective, coronary risk, and atherogenic indexes. *In* high amounts, *T. catappa* contains total phenolic compounds, flavonoids, cardiac glycosides, alkaloids, and saponins, act individually or synergistically to elicit antioxidant activities that may manifest in the form of anti-atherosclerotic effects.

New biomarkers in atherosclerosis

Atherosclerosis is recognized as an energy-imbalanced metabolic disease.[9] The pathogenesis of atherosclerosis is connected to hyperlipidemia/hypercholesteremia-induced unwavering energy disturbances, inflammation, and oxidative stress. It is unarguable that atherosclerosis also occurs in some patients whose lipid level is well-controlled, suggesting that other pathogenic factors may contribute to the phenomenon. The direct and indirect protein interactions constitute a functional association of an essential survival complex in the aorta, heart, and liver.

The assembly of all known and unknown proteins and the genetic association in the cell results in a protein network of proteome-wide functional connectivity. Thus, the protein network is an ideal scaffold for data integration, visualization, and biomarker discovery. In addition, an in-depth understanding of the molecular mechanism of the disease requires knowledge of all functional integration between the expressed proteins and metabolites.

β-actin (ACTB) as a main switch of atherosclerosis

Unexpectedly, the current protein interactome demonstrated that β-actin could be a central regulator of atherosclerosis through more than 84 connectomes, including VCL (vinculin), GAPDH (glyceraldehyde 3-phosphate dehydrogenase), ANXA5 (annexin A5), PARVA (α-parvin), ILK (integrin-like protein kinase), WAS (wasp actin nucleation factor), MSN (moesin), and ACTN2 (α-actinin 2). (Fig. 3, Supporting Information Table S1).[26] β-actin and EGFR are connected to nitric oxide metabolism.[27]

Nitric oxide synthase 2A (NOS2, inducible nitric oxide synthase) is connected to MYD88, fatty acid binding protein 5, and IL1B.[28] Besides, phosphorylation regulators, including CCNA (cyclin A1), CDK2,

CRK, and TICAM1, were also connected to NOS2A to respond to the intracellular concentration of nitric oxide.[29]

For artery homeostasis, nitric oxide synthase (NOS) regulates the cell's nitric oxide (NO) concentration. NO maintains vascular structure by inhibiting blood clotting, preventing vascular smooth muscle cells (SMCs) from over-proliferation. NO controls basal blood flow, vascular integrity, superoxide scavenging, and protein nitration. Inducible NOS in immune cells, typically stimulated under oxidative stress, generates a high NO level that can be cytotoxic and proinflammatory.

NO is angiogenic through enhancing endothelial migration and inducing reorganization of extracellular matrix (ECM) proteins.[30] NOS uncoupling caused by an insufficient substance (oxygen and arginine) abrogates NO generation property.

The current interactome suggests that atherosclerosis also shows characteristics consistent with chronic inflammation. Enhanced immune cells and elevated proinflammatory proteins result in structural and functional changes in the aorta, heart, and liver.

Positive correlation between cystic fibrosis and atherosclerosis

The current map demonstrated that atherosclerosis is connected to cystic fibrosis through CFTR (cystic fibrosis transmembrane conductance regulator).[31] CFTR is an epithelial ion channel vital in regulating epithelial ions, including chloride, water transport, and fluid homeostasis, linked to ATP hydrolysis. CFTR is permeable to HCO_3^- and the selectivity depends on the extracellular chloride concentration. CFTR controls cystic fibrosis and atherosclerosis through transcription, energy, and inflammation through critical regulators, including p53, GAPDH, CDH1, IL1B, MSN, CBL, ACTB, and SLC9A3R1.[32] Cystic fibrosis and atherosclerosis share common risk factors, including a high-fat diet, increased oxidative stress, chronic inflammation, altered lipid metabolism, and diabetes. In addition, both conditions show endothelial dysfunction and increased vascular stiffness. Studies suggest chronic inflammation induces vascular disease through endothelial injury and increased arterial stiffness mechanism.

Thrombosis, atherosclerosis, and plaque rupture

Next, we dissected the atherosclerosis mechanism based on thrombosis and plaque rupture.[33] HRG (histidine-rich glycoprotein) binds several thrombosis-related ligands, including heme, heparin, heparan sulfate, thrombospondin, plasminogen, and divalent metal ions.[34] HRG binds heparin and glycosaminoglycans in a zinc-dependent manner and heparan sulfate on the surface of the liver, lung, kidney, and heart endothelial cells. The N-sulfated polysaccharide chain-HRG complex on the surface of liver endothelial cells acts as an immune complex. An atherosclerotic plaque rupture exposes necrotic core components to the circulation to generate a fibrin monolayer as a coagulation cascade. Subsequently, circulating platelets and inflammasome lead to platelet activation and atherothrombosis.

Macrophage balance and atherosclerosis

Atherosclerosis begins with an early inflammatory reaction, including an imbalance in energy metabolism and an immune response induced by macrophages in the artery.[35] The current interactome map suggests that macrophage balance could initiate atherosclerosis.

Our interactome map shows that macrophage-related proteins, including CHI3L1, HBEGF, IL1A, ITGAM, and NOS2, are related to atherosclerosis at the molecular level.[36]

CHI3L1 (chitinase-3-like protein 1) has no chitinase activity; however, it plays a role in tissue remodeling to respond to environmental changes.

HBEGF (heparin-binding EGF-like growth factor) is connected to EGFR, ERBB2, and ERBB4.[37] It is necessary for normal cardiac valve formation, heart function, and macrophage-mediated cellular proliferation. HBEGF is a more potent mitogen for smooth muscle cells than EGF, showing higher affinity toward EGF receptor, compared to EGF.

Activated macrophages produce IL1A (interleukin-1 alpha). IL-1 induces IL-2 release, stimulating thymocyte proliferation, fibroblast growth factor activity, and B-cell maturation. IL-1 proteins are involved in the inflammatory response, identified as endogenous pyrogens, and stimulate the release of prostaglandin and collagenase from synovial cells.

ITGAM (integrin alpha-M) is implicated in adhesive interactions of monocytes, macrophages, and granulocytes and in mediating the uptake of complement-coated particles.[38] It is identical to CR-3, the receptor for the iC3b fragment of the third complement component. It recognizes the R-G-D peptide in C3b. ITGAM is also a receptor for fibrinogen, factor X, and ICAM1. It recognizes the P1 and P2 peptides of the fibrinogen gamma chain and regulates neutrophil migration. NOS2 (inducible nitric-oxide synthase) generates nitric oxide (NO), a protein nitration and peroxynitrite synthesis messenger molecule. NOS has nitrosylase activity to mediate cysteine nitrosylation of cytoplasmic target proteins, including PTGS2 and COX2. As a component of the iNOS-S100A8/9 transnitrosylase complex involved in the selective inflammatory stimulus-dependent S-nitrosylation of GAPDH on Cys-247 implicated in the regulation of the GAIT complex activity.[39]

Energy imbalance due to altered lipid/glucose homeostasis

The protein interactome map demonstrated that specific correlations might exist between lipid and glucose metabolism shown by the interconnection of APOE, CBL, CCND2, CDH1, CDKN1B, CFTR, cathepsin 5, EGF, GAPDH, glucose phosphate isomerase, fatty acid binding protein 5, and pro-platelet basic protein (Supporting Information Table S1, S2).

Citric acid is the center of energy metabolism, responding to energy demands dynamically under chronic oxidative stress.[40] Inflammatory stimuli activate the macrophages, and two breakpoints in the TCA cycle lead to the accumulation of intermediates. The citric acid in the TCA cycle in the macrophage under inflammatory stimulation plays an essential role in the progression of atherosclerosis.[41] A central hub of

carbon metabolism in atherosclerosis consists of crucial elements, including ACTB, ITGAM, APOB, APOE, SERPINE1, STAT3, p53, TLR3, MYD88, and CDK2.[42]

In conclusion, using a diet-induced atherosclerosis rat model, the current study tested the hypothesis of the anti-atherosclerotic a roles of *Terminalia catappa* fruit extracts. Histological examinations demonstrated that the aorta, heart, and liver improved cholesterol deposits in the lumen of the blood vessels. Treatment with *Terminalia catappa* extracts demonstrated an improved histopathology., lipid profile, enzyme biomarkers, cardioprotective index, and atherogenic index. The current study will guide further investigation to propose a clinical application to treat vessel diseases, including atherosclerosis.[43]

Declarations

Authors' contributions

Doris Tabansi participated in research design, experimental performance, manuscript drafting, and data analysis. Daniel Dahiru participated in the research design, manuscript preparation, and revision. Ambrose Teru Patrick participated in research design, technical assistance, and manuscript preparation. Faith Pwaniyibo Samson participated in data analysis, manuscript preparation, and revision. Wan Jin Jahng participated in research design, data analysis, manuscript preparation, and revision. All authors wrote, read, and approved the final manuscript.

Email: ddchidama72@mautech.edu.ng, Phone No: +234 802 552 6252

Email: patrickteruambrose@chosun.kr, Phone No: +8210 4865 2322

Email: samsonfaith0@chosun.kr, Phone No: +8210 7495 6733

Funding

Development Administration's Regional Specialized Crop Technology Development Project with the Development and field validation of a postharvest management manual for exported persimmons (project number PJ01696801). In addition, the current study was supported in part by funding from Sweet Persimmon Research Institute, Gyeongsangnamdo Agricultural Research and Extension Services, Korea, and Julia Laboratory.

Conflict of interest

The authors declare there are no competing interests.

Ethics approval and consent to participate

The Institutional Animal Care and Use Committee of the Modibbo Adama University of Technology Yola approved all animal protocols.

Consent for publication

Not applicable.

Availability of data and materials

The current manuscript and its supplementary information files include all data generated or analyzed during this study.

References

1. Chandran, M.; S, S.; Abhirami; Chandran, A.; Jaleel, A.; Plakkal Ayyappan, J. Defining atherosclerotic plaque biology by mass spectrometry-based omics approaches. *Mol Omics* **2023**, *19* (1), 6-26. DOI: 10.1039/d2mo00260d From NLM Medline.
2. Tucureanu, M. M.; Filippi, A.; Alexandru, N.; Ana Constantinescu, C.; Ciortan, L.; Macarie, R.; Vadana, M.; Voicu, G.; Frunza, S.; Nistor, D.; et al. Diabetes-induced early molecular and functional changes in aortic heart valves in a murine model of atherosclerosis. *Diab Vasc Dis Res* **2019**, *16* (6), 562-576. DOI: 10.1177/1479164119874469 From NLM Medline.
3. Birjmohun, R. S.; Kees Hovingh, G.; Stroes, E. S.; Hofstra, J. J.; Dallinga-Thie, G. M.; Meijers, J. C.; Kastelein, J. J.; Levi, M. Effects of short-term and long-term danazol treatment on lipoproteins, coagulation, and progression of atherosclerosis: two clinical trials in healthy volunteers and patients with hereditary angioedema. *Clin Ther* **2008**, *30* (12), 2314-2323. DOI: 10.1016/j.clinthera.2008.12.021 From NLM Medline.
4. Mauriello, A.; Servadei, F.; Sangiorgi, G.; Anemona, L.; Giacobbi, E.; Liotti, D.; Spagnoli, L. G. Asymptomatic carotid plaque rupture with unexpected thrombosis over a non-canonical vulnerable lesion. *Atherosclerosis* **2011**, *218* (2), 356-362. DOI: 10.1016/j.atherosclerosis.2011.06.056 From NLM Medline.
5. Niimi, M.; Keyamura, Y.; Nozako, M.; Koyama, T.; Kohashi, M.; Yasufuku, R.; Yoshikawa, T.; Fan, J. Probucol inhibits the initiation of atherosclerosis in cholesterol-fed rabbits. *Lipids Health Dis* **2013**, *12*, 166. DOI: 10.1186/1476-511X-12-166 From NLM Medline.
6. Mandraffino, G.; Morace, C.; Franze, M. S.; Nassisi, V.; Sinicropi, D.; Cinquegrani, M.; Saitta, C.; Scoglio, R.; Marino, S.; Belvedere, A.; et al. Fatty Liver as Potential Biomarker of Atherosclerotic Damage in Familial Combined Hyperlipidemia. *Biomedicines* **2022**, *10* (8). DOI: 10.3390/biomedicines10081770 From NLM PubMed-not-MEDLINE.
7. Mehu, M.; Narasimhulu, C. A.; Singla, D. K. Inflammatory Cells in Atherosclerosis. *Antioxidants (Basel)* **2022**, *11* (2). DOI: 10.3390/antiox11020233 From NLM PubMed-not-MEDLINE.
8. Chen, J.; Su, Y.; Pi, S.; Hu, B.; Mao, L. The Dual Role of Low-Density Lipoprotein Receptor-Related Protein 1 in Atherosclerosis. *Front Cardiovasc Med* **2021**, *8*, 682389. DOI: 10.3389/fcvm.2021.682389 From NLM PubMed-not-MEDLINE.

9. Stancu, C. S.; Toma, L.; Sima, A. V. Dual role of lipoproteins in endothelial cell dysfunction in atherosclerosis. *Cell Tissue Res* **2012**, *349* (2), 433-446. DOI: 10.1007/s00441-012-1437-1 From NLM Medline.
10. Davidson, M. H.; Gandhi, S. K.; Ohsfeldt, R. L.; Fox, K. M. Hypercholesterolemia treatment patterns and low-density lipoprotein cholesterol monitoring in patients with a diagnosis of atherosclerosis in clinical practice. *Am J Med* **2009**, *122* (1 Suppl), S51-59. DOI: 10.1016/j.amjmed.2008.10.017 From NLM Medline.
11. Georgia-Eirini, D.; Athina, S.; Wim, V. B.; Christos, K.; Theodoros, C. Natural Products from Mediterranean Diet: From Anti-hyperlipidemic Agents to Dietary Epigenetic Modulators. *Curr Pharm Biotechnol* **2019**, *20* (10), 825-844. DOI: 10.2174/1573407215666190628150921 From NLM Medline.
12. Umoren, E.; Asiwe, J. N.; Okon, I. A.; Levi Amangieka, A.; Nyenke, C. U.; Nnamudi, A. C.; Modo, E. U.; Bassey, A. I. L.; Nwikue, G.; Etim, O. E. Terminalia catappa attenuates phenylhydrazine-induced anaemia and hepato-renal toxicity in male Wistar rat by boosting blood cells, modulation of lipoproteins and up-regulation of in vivo antioxidant armouries. *Biomarkers* **2023**, 1-11. DOI: 10.1080/1354750X.2023.2166588 From NLM Publisher.
13. Gao, H.; Song, R. J.; Jiang, H.; Zhang, W.; Han, S. F. Oat fiber supplementation alleviates intestinal inflammation and ameliorates intestinal mucosal barrier via acting on gut microbiota-derived metabolites in LDLR(-/-) mice. *Nutrition* **2022**, *95*, 111558. DOI: 10.1016/j.nut.2021.111558 From NLM Medline.
14. Almofti, M. R.; Huang, Z.; Yang, P.; Rui, Y.; Yang, P. Proteomic analysis of rat aorta during atherosclerosis induced by high cholesterol diet and injection of vitamin D3. *Clin Exp Pharmacol Physiol* **2006**, *33* (4), 305-309. DOI: 10.1111/j.1440-1681.2006.04366.x From NLM Medline.
15. Lehnen, M.; Ebert, B. E.; Blank, L. M. A comprehensive evaluation of constraining amino acid biosynthesis in compartmented models for metabolic flux analysis. *Metab Eng Commun* **2017**, *5*, 34-44. DOI: 10.1016/j.meteno.2017.07.001 From NLM PubMed-not-MEDLINE.
16. Herrington, D. M.; Mao, C.; Parker, S. J.; Fu, Z.; Yu, G.; Chen, L.; Venkatraman, V.; Fu, Y.; Wang, Y.; Howard, T. D.; et al. Proteomic Architecture of Human Coronary and Aortic Atherosclerosis. *Circulation* **2018**, *137* (25), 2741-2756. DOI: 10.1161/CIRCULATIONAHA.118.034365 From NLM Medline.
17. Nair, J.; Ghatge, M.; Kakkar, V. V.; Shanker, J. Network analysis of inflammatory genes and their transcriptional regulators in coronary artery disease. *PLoS One* **2014**, *9* (4), e94328. DOI: 10.1371/journal.pone.0094328 From NLM Medline.
18. Taylor, E.; Huang, N.; Bodde, J.; Ellison, A.; Killiany, R.; Bachschmid, M. M.; Hamilton, J. MRI of atherosclerosis and fatty liver disease in cholesterol fed rabbits. *J Transl Med* **2018**, *16* (1), 215. DOI: 10.1186/s12967-018-1587-3 From NLM Medline.
19. Hermjakob, H.; Montecchi-Palazzi, L.; Bader, G.; Wojcik, J.; Salwinski, L.; Ceol, A.; Moore, S.; Orchard, S.; Sarkans, U.; von Mering, C.; et al. The HUPO PSI's molecular interaction format--a community

standard for the representation of protein interaction data. *Nat Biotechnol* **2004**, *22* (2), 177-183. DOI: 10.1038/nbt926 From NLM Medline.

20. Zhou, G.; Pang, Z.; Lu, Y.; Ewald, J.; Xia, J. OmicsNet 2.0: a web-based platform for multi-omics integration and network visual analytics. *Nucleic Acids Res* **2022**, *50* (W1), W527-533. DOI: 10.1093/nar/gkac376 From NLM Publisher.
21. Fleming, C. A.; Mohan, H. M.; O'Leary, D. P.; Corrigan, M.; Redmond, H. P. Metabolomic Pathway Activity with Genomic Single-Nucleotide Polymorphisms Associated with Colorectal Cancer Recurrence and 5-Year Overall Survival. *J Gastrointest Cancer* **2022**. DOI: 10.1007/s12029-022-00813-3 From NLM Publisher.
22. Rajamannan, N. M. Atorvastatin Attenuates Bone Loss and Aortic Valve Atheroma in LDLR Mice. *Cardiology* **2015**, *132* (1), 11-15. DOI: 10.1159/000381703 From NLM Medline.
23. Rossetti, C.; Laraia, L. Thermal Proteome Profiling Reveals Distinct Target Selectivity for Differentially Oxidized Oxysterols. *ACS Chem Biol* **2022**, *17* (7), 1677-1684. DOI: 10.1021/acschembio.2c00383 From NLM Medline.
24. Sobenin, I. A.; Andrianova, I. V.; Lakunin, K. Y.; Karagodin, V. P.; Bobryshev, Y. V.; Orekhov, A. N. Anti-atherosclerotic effects of garlic preparation in freeze injury model of atherosclerosis in cholesterol-fed rabbits. *Phytomedicine* **2016**, *23* (11), 1235-1239. DOI: 10.1016/j.phymed.2015.10.014 From NLM Medline.
25. Luirink, I. K.; Hutten, B. A.; Greber-Platzer, S.; Kolovou, G. D.; Dann, E. J.; de Ferranti, S. D.; Taylan, C.; Bruckert, E.; Saheb, S.; Oh, J.; et al. Practice of lipoprotein apheresis and short-term efficacy in children with homozygous familial hypercholesterolemia: Data from an international registry. *Atherosclerosis* **2020**, *299*, 24-31. DOI: 10.1016/j.atherosclerosis.2020.01.031 From NLM Medline.
26. Wang, R.; Wang, Z.; Jiang, L.; Gu, G.; Zheng, B.; Xian, L.; Zhang, Y.; Wang, J. High Actin Expression in Thrombus of Acute Ischemic Stroke Can Be a Biomarker of Atherothrombotic Origin Stroke. *Front Neurol* **2022**, *13*, 896428. DOI: 10.3389/fneur.2022.896428 From NLM PubMed-not-MEDLINE.
27. Brenner, C.; Galluzzi, L.; Kepp, O.; Kroemer, G. Decoding cell death signals in liver inflammation. *J Hepatol* **2013**, *59* (3), 583-594. DOI: 10.1016/j.jhep.2013.03.033 From NLM Medline.
28. Baumann, A.; Burger, K.; Brandt, A.; Staltner, R.; Jung, F.; Rajcic, D.; Lorenzo Pisarello, M. J.; Bergheim, I. GW9662, a peroxisome proliferator-activated receptor gamma antagonist, attenuates the development of non-alcoholic fatty liver disease. *Metabolism* **2022**, *133*, 155233. DOI: 10.1016/j.metabol.2022.155233 From NLM Medline.
29. Maejima, Y.; Adachi, S.; Ito, H.; Nobori, K.; Tamamori-Adachi, M.; Isobe, M. Nitric oxide inhibits ischemia/reperfusion-induced myocardial apoptosis by modulating cyclin A-associated kinase activity. *Cardiovasc Res* **2003**, *59* (2), 308-320. DOI: 10.1016/s0008-6363(03)00425-5 From NLM Medline.
30. Jannatbabaei, A.; Tafazzoli-Shadpour, M.; Seyedjafari, E. Effects of substrate mechanics on angiogenic capacity and nitric oxide release in human endothelial cells. *Ann N Y Acad Sci* **2020**, *1470* (1), 31-43. DOI: 10.1111/nyas.14326 From NLM Medline.

31. Li, Z.; Shen, Z.; Xue, H.; Cheng, S.; Ji, Q.; Liu, Y.; Yang, X. CFTR protects against vascular inflammation and atherogenesis in apolipoprotein E-deficient mice. *Biosci Rep* **2017**, *37* (4). DOI: 10.1042/BSR20170680 From NLM Medline.
32. Lu, Y. C.; Chen, H.; Fok, K. L.; Tsang, L. L.; Yu, M. K.; Zhang, X. H.; Chen, J.; Jiang, X.; Chung, Y. W.; Ma, A. C.; et al. CFTR mediates bicarbonate-dependent activation of miR-125b in preimplantation embryo development. *Cell Res* **2012**, *22* (10), 1453-1466. DOI: 10.1038/cr.2012.88 From NLM Medline.
33. Suades, R.; Padro, T.; Vilahur, G.; Badimon, L. Platelet-released extracellular vesicles: the effects of thrombin activation. *Cell Mol Life Sci* **2022**, *79* (3), 190. DOI: 10.1007/s00018-022-04222-4 From NLM Medline.
34. Wang, Y.; Xu, L. Y.; Lam, K. S.; Lu, G.; Cooper, G. J.; Xu, A. Proteomic characterization of human serum proteins associated with the fat-derived hormone adiponectin. *Proteomics* **2006**, *6* (13), 3862-3870. DOI: 10.1002/pmic.200500840 From NLM Medline.
35. Eligini, S.; Gianazza, E.; Mallia, A.; Ghilardi, S.; Banfi, C. Macrophage Phenotyping in Atherosclerosis by Proteomics. *Int J Mol Sci* **2023**, *24* (3). DOI: 10.3390/ijms24032613 From NLM Medline.
36. Gong, Z.; Xing, S.; Zheng, F.; Xing, Q. Increased expression of chitinase 3-like 1 in aorta of patients with atherosclerosis and suppression of atherosclerosis in apolipoprotein E-knockout mice by chitinase 3-like 1 gene silencing. *Mediators Inflamm* **2014**, *2014*, 905463. DOI: 10.1155/2014/905463 From NLM Medline.
37. Zhou, Z. N.; Sharma, V. P.; Beaty, B. T.; Roh-Johnson, M.; Peterson, E. A.; Van Rooijen, N.; Kenny, P. A.; Wiley, H. S.; Condeelis, J. S.; Segall, J. E. Autocrine HBEGF expression promotes breast cancer intravasation, metastasis and macrophage-independent invasion in vivo. *Oncogene* **2014**, *33* (29), 3784-3793. DOI: 10.1038/onc.2013.363 From NLM Medline.
38. da Silva, K. S.; Pinto, P. R.; Fabre, N. T.; Gomes, D. J.; Thieme, K.; Okuda, L. S.; Iborra, R. T.; Freitas, V. G.; Shimizu, M. H. M.; Teodoro, W. R.; et al. N-acetylcysteine Counteracts Adipose Tissue Macrophage Infiltration and Insulin Resistance Elicited by Advanced Glycated Albumin in Healthy Rats. *Front Physiol* **2017**, *8*, 723. DOI: 10.3389/fphys.2017.00723 From NLM PubMed-not-MEDLINE.
39. Lu, Y.; Song, W.; Li, Y.; Xiao, J.; Du, K.; Fu, Q.; Zhang, Y.; Zhao, L.; Yin, Y.; Hu, T.; et al. Mechanisms of NO-Mediated Protein S-Nitrosylation in the Lens-Induced Myopia. *Oxid Med Cell Longev* **2022**, *2022*, 8296043. DOI: 10.1155/2022/8296043 From NLM In-Process.
40. Quijano, C.; Trujillo, M.; Castro, L.; Trostchansky, A. Interplay between oxidant species and energy metabolism. *Redox Biol* **2016**, *8*, 28-42. DOI: 10.1016/j.redox.2015.11.010 From NLM Medline.
41. Liang, Y.; Chen, Y.; Li, L.; Zhang, S.; Xiao, J.; Wei, D. Krebs Cycle Rewired: Driver of Atherosclerosis Progression? *Curr Med Chem* **2022**, *29* (13), 2322-2333. DOI: 10.2174/0929867328666210806105246 From NLM Medline.
42. Park, J. Y.; Seong, J. K.; Paik, Y. K. Proteomic analysis of diet-induced hypercholesterolemic mice. *Proteomics* **2004**, *4* (2), 514-523. DOI: 10.1002/pmic.200300623 From NLM Medline.

43. Ntchapda, F.; Djedouboum, A.; Talla, E.; Sokeng Dongmo, S.; Nana, P.; Adjia, H.; Nguimbou, R. M.; Bonabe, C.; Gaimatakon, S.; Njintang Yanou, N.; et al. Hypolipidemic and anti-atherogenic effect of aqueous extract leaves of Ficus glumosa (Moraceae) in rats. *Exp Gerontol* **2015**, *62*, 53-62. DOI: 10.1016/j.exger.2014.12.015 From NLM Medline.

Figures

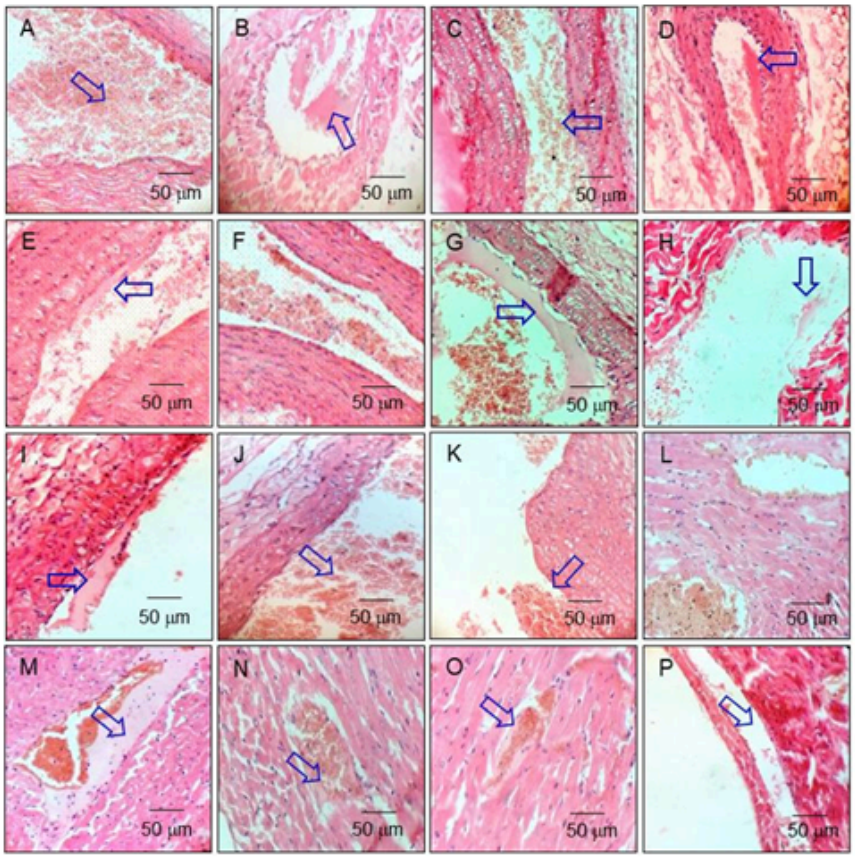

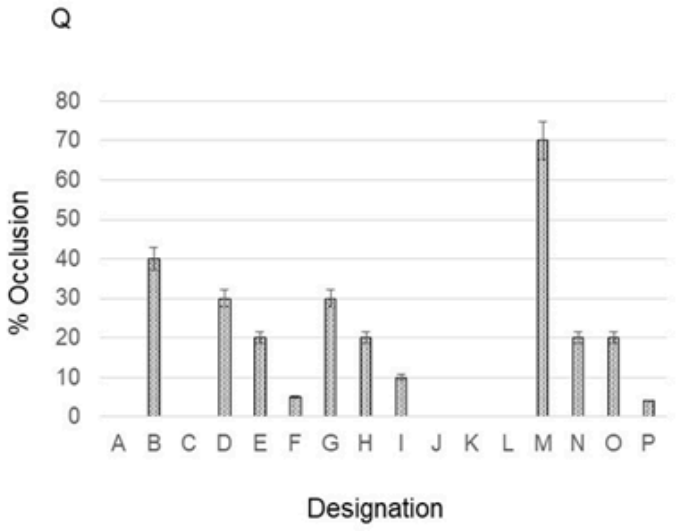

Figure 1

The aorta, heart, and liver tissues were examined histologically using hematoxylin and eosin staining (H&E) under the atherogenic diet/plant extracts-treated conditions (scale bar=50 mm). Standard diet showed a free lumen containing blood cells and intima of the endothelium without any lipid deposit (A). The atherogenic conditions occlude over 40 % of blood passage by lipid plaques (B). Atorvastatin (10 mg/kg) was used as positive control and demonstrated much-decreased cholesterol deposits (C). *Terminalia catappa*extracts (100 mg/kg ethanol extract) under an atherogenic condition showed cholesterol plaques and clusters (D). A dose-dependent effect was observed when a higher concentration of *Terminalia catappa* (200 mg/kg ethanol extracts) showed fewer cholesterol plaques (E). The highest concentration of *Terminalia catappa* (300mg/kg of ethanol extracts) indicated much-decreased levels (F). Co-administration of *Terminalia catappa* aqueous extracts (100 mg/kg ATC) and atherogenic diet showed cholesterol plaques and blood cell clusters (G). Aqueous extracts with an atherogenic diet (200 mg/kg ATC) show fewer cholesterol plaques (H). The highest concentrations of *Terminalia catappa*(300mg/kg ATC) showed much-decreased cholesterol plaques (I). *Terminalia catappa*-only treatment showed no lipid deposits in their intima (J, 300 mg/kg ETC; K, 300 mg/kg ATC). Under the standard diet condition, healthy cardiac tissue showed free blood cells and no lipid deposits (L). Heart sections under the atherogenic condition showed massive cholesterol plaques (M). *Terminalia catappa* (100 mg/kg ETC) showed milder cholesterol plaques and blood cell clusters in the lumen (N). Dose-dependent (200 m/kg ETC) anti-atherosclerotic effects of Terminalia catappa were observed with much-reduced cholesterol plaques and blood cell clusters (O). The highest dose of *Terminalia catappa* (300 mg/kg ETC) shows minimum cholesterol plaques in the coronary artery (P). Quantitative analysis of *Terminalia catappa*-treated tissues (Q). The Y-axis represents % occlusion, whereas the X-axis shows the designation of each condition.

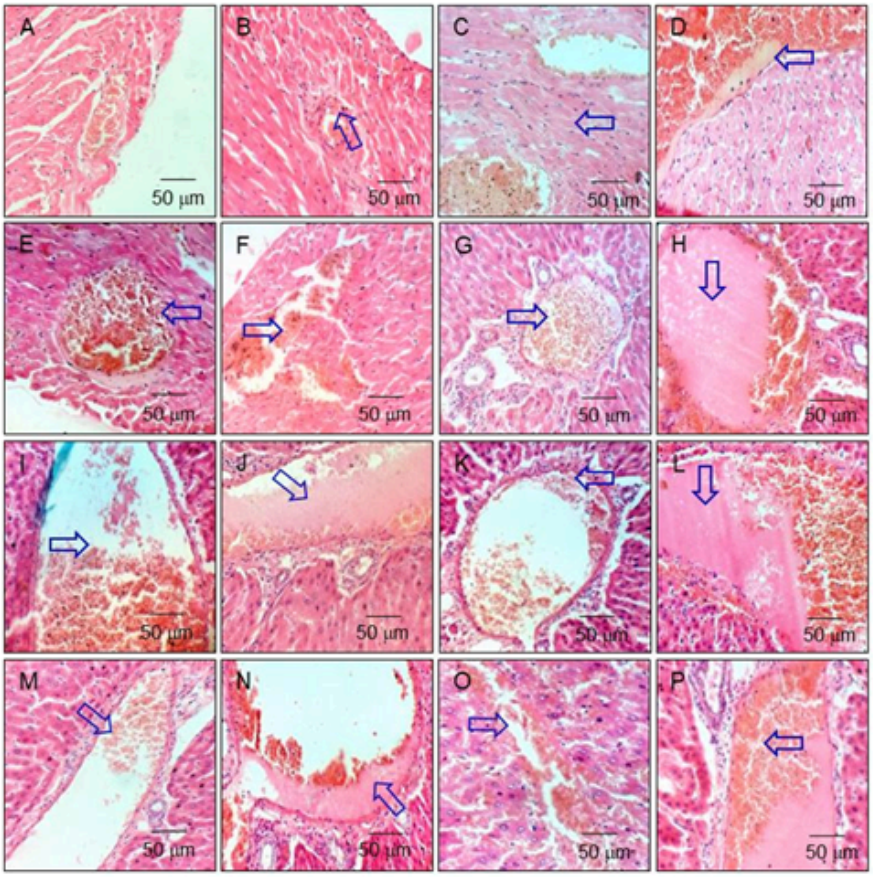

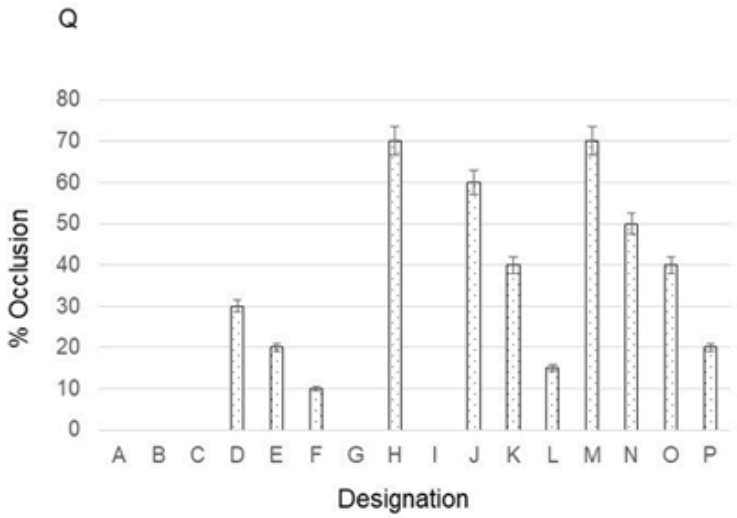

Figure 2

Terminalia catappa extracts treatment under standard diet conditions showed healthy cardiac tissue (A. 300 mg/kg ETC; B. 300 mg/kg ATC), similar to a stand diet-only condition (C) (scale bar=50 mm). Plant extracts (100 mg/kg ATC) with an atherogenic diet show cardiac tissue with coronary arteries containing mild cholesterol plaques and blood cell clusters in the lumen (D). An increased dose of plant extracts (200 mg/kg ATC with an atherogenic diet) shows cholesterol plaques occluding 20 % of blood passage

(E). The highest dose (300 mg/kg) shows much-reduced occlusion of blood passage (F). Under the standard diet, the liver shows healthy hepatocyte tissue with blood vessels containing blood cells within the lumen (G). Atherogenic diet-induced massive deposits of cholesterol plaques in the lumen with 70% occlusion of blood passage (H). Concomitant administration of Atorvastatin (10 mg/kg, positive control) with an atherogenic diet shows no cholesterol deposits; however, blood cell clusters exist in the lumen (I). Ethanol extracts (100 mg/kg) with an atherogenic diet show moderate cholesterol plaques and blood clusters in the lumen (J). Decreased cholesterol plaques were observed with the 200 mg/kg ETC/atherogenic diet group (K). The highest dose (300 mg/kg ETC) decreased cholesterol plaques and improved blood passage from 15% to 85% (L). Atherogenic diet-induced massive deposits of cholesterol plaques in the lumen with 70% occlusion of blood passage (H). Aqueous extracts (ATC 100 mg/kg) with an atherogenic diet show cholesterol plaques and blood cell clusters in the lumen (N). ATC (200 mg/kg) with an atherogenic diet shows cholesterol plaques occluding 20 % of blood passage (O). The highest dose of ATC (300 mg/kg) with an atherogenic diet shows healthier liver tissue with much fewer lipid deposits (P). Quantitative analysis of *Terminalia catappa*-treated tissues (Q). The Y-axis represents % occlusion, whereas the X-axis shows the designation of each condition.

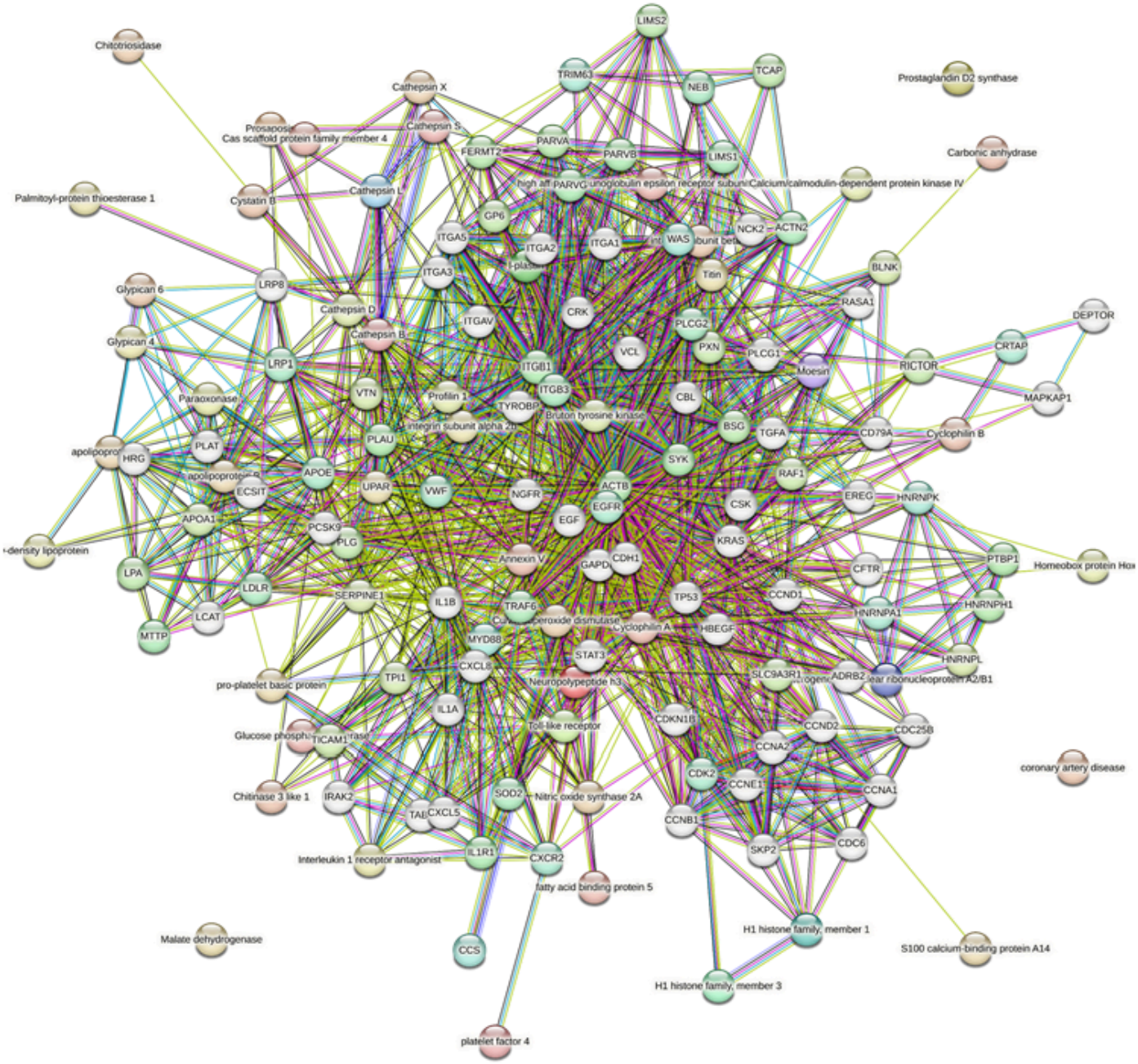

Figure 3

The atherosclerosis interactome was established using STRING software. The protein interactome map demonstrated that atherosclerosis-related proteins might influence energy imbalance, inflammation, cell cycle, cystic fibrosis, lipid concentration, and phosphorylation signaling when upregulated or downregulated under various stress conditions. The atherosclerosis-specific proteins in the map were divided into six groups based on their functional regulatory roles, including k-means clustering. Protein interactome was dissected into six different subnetworks; (A) podosome/macrophage (green; PARV, WAS, ITGA), (B) lipid metabolism (red; APOE, LPA, LCAT, APOA1, LRP1), (C) transcription control (blue; EGFR, PLCG, TRAF6, annexin V, MYD88, STAT3, p53), (D) anion channel/salt concentration/cystic fibrosis

(pink; CFTR, EREG, RICTOR), (E) inflammation switch (yellow; IL1A, ICAM1, NOS, FABP, TLR), (F) cell cycle (black; CCNA2, CDK2, CDC6).

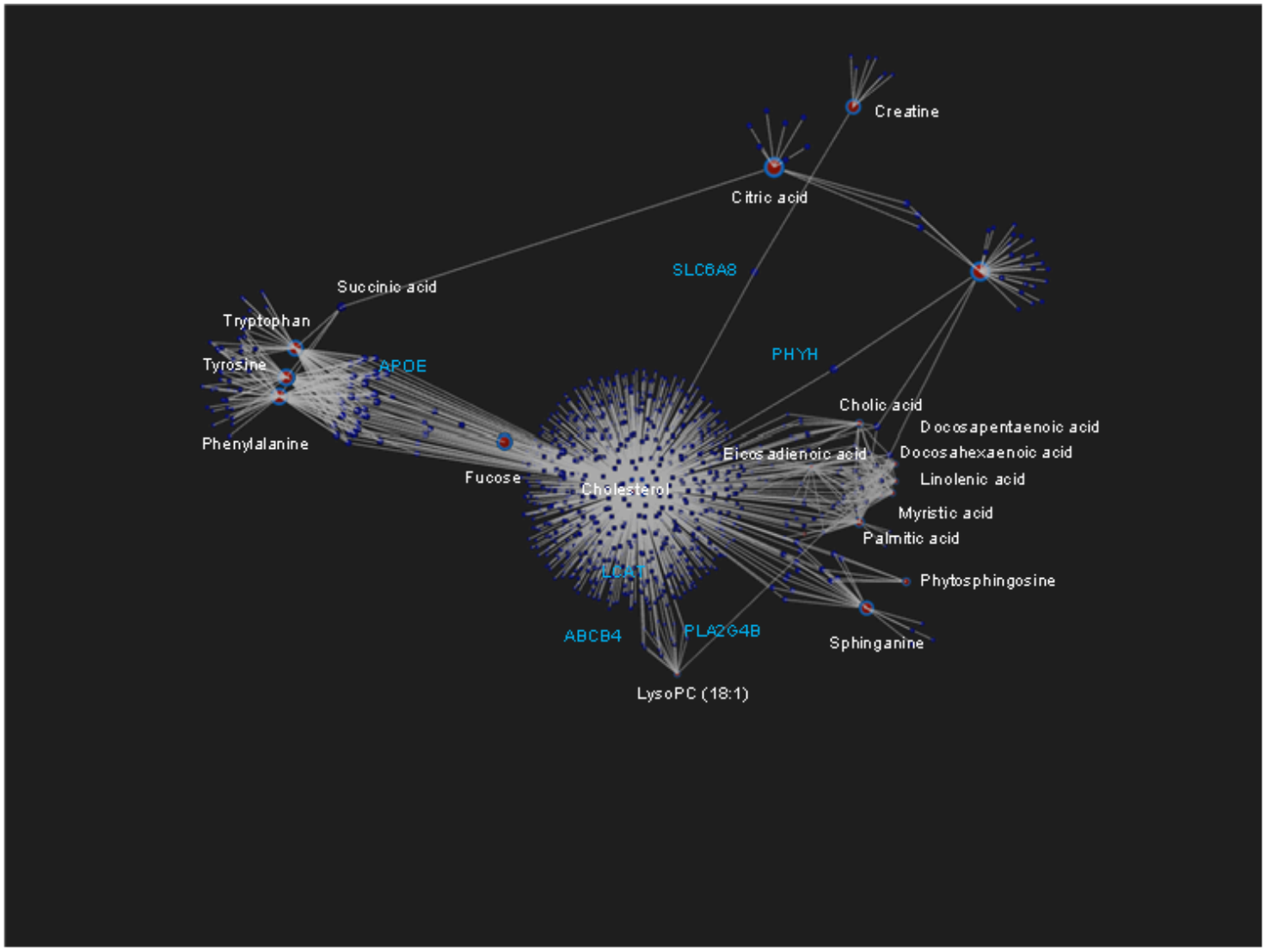

Figure 4

The metabolome map was established using various bioinformatic tools, including OmicsNet software. The metabolome map demonstrated that atherosclerotic metabolites were interconnected to the citric acid cycle, amino acid metabolism, lysoPC, cholesterol, cholic acid, succinic acid, and creatine.

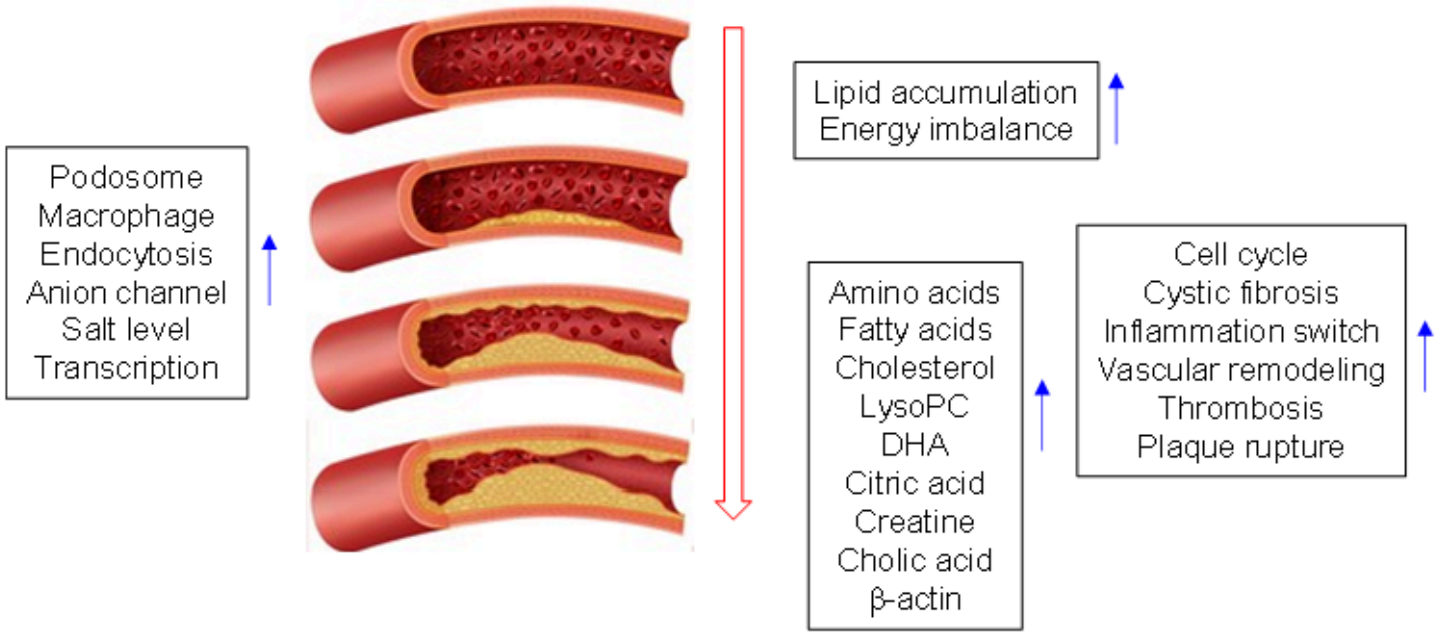

Figure 5

The protein interactome and metabolome map demonstrated that potential atherosclerosis mechanisms might include fatty acids (palmitic acid, linolenic acid, DHA), altered aromatic amino acids (phenylalanine, tyrosine, tryptophan), organic acid metabolism (succinic acid, citric acid, cholic acid), sphingolipid (sphinganine, phytosphingosine), and cholesterol.

Supplementary Files

This is a list of supplementary files associated with this preprint. Click to download.

- SUPPORTINGINFORMATIONFIGURES1KMEANSCLUSTERING.pdf
- SUPPORTINGINFORMATIONTABLES1PROTEOMEMAPPING.pdf
- SUPPORTINGINFORMATIONTABLES2PROTEINDESCRIPTION.pdf
- SUPPORTINGINFORMATIONTABLES3DOMAINSUMMARY.pdf
- SUPPORTINGINFORMATIONTABLES4KMEANSCLUSTERING.pdf
- SUPPORTINGINFORMATIONTABLES5METABOLOMICSATHEROSCLEROSIS.pdf
- SUPPORTINGINFORMATIONTABLES6.pdf
- SUPPORTINGINFORMATIONTABLES7.pdf
- GA.png